A null test for null correctors: error analysis

Jim Burge
Steward Observatory Mirror Laboratory, University of Arizona
Tucson, Arizona 85721

ABSTRACT

An optical test has been devised to test and qualify null correctors that are used for measuring highly aspheric primary mirrors. The technique employs a rotationally symmetric computer-generated hologram (CGH) that tests the null corrector directly by synthesizing a wavefront that would be returned by a perfect primary mirror. A description of the test and summary of the error analysis are given. The error analysis includes hologram errors from pattern distortion, substrate flatness, and etch depth variations. It also includes the effects of errors in the wavelength and data analysis errors. This resulting analysis shows ±78 ppm accuracy for measuring the conic constant of null correctors built for measuring 3.5-m *f*/1.75 primary mirrors.

1. INTRODUCTION

Aspheric optical surfaces are often measured using null correctors to allow a null interferometric test. Since the optical surfaces are fabricated based on the results of the test, the null correctors define the shapes of the final optics. There is always a possibility that the null corrector could be flawed, resulting in the final shape of the optic being incorrect. Two recent telescopes had their primary mirrors made to the wrong shape because of errors in the null correctors -- the Hubble Space Telescope[1] and the European New Technology Telescope[2]. If accurate testing of the null correctors had been performed, the errors would have been discovered and corrected in the shop. Instead, the errors were not discovered until the finished mirrors were in their operational telescopes.

A new, highly accurate test for null correctors is described that uses circularly symmetric computer-generated holograms. This paper gives a general description and error analysis of this new method of testing null correctors. The derivations are given more completely by Burge[3], also the results and more detailed analyses of actual measurements are given in another paper[4]. Some useful background information on CGH and optical testing is given in Section 2. The design and fabrication of the hologram are described in Section 3. An error analysis is presented in Section 4 that includes errors in the fabrication of the CGH, errors in performing the test, and errors in the data analysis. The CGH null lens test was successfully performed on null correctors for two 3.5-m *f*/1.75 primary mirrors, and the error analysis for these tests is given as an example in Section 5.

In the CGH null lens test, a computer-generated hologram of the mirror is tested by the null lens. The hologram is made so it will appear to the test lenses as if it were a perfect primary mirror. The test is insensitive to alignment errors, and uses no optics other than the hologram. The hologram is designed and fabricated independently from the null corrector, so agreement between the two indicates a high probability that both are correct.

The hologram is simply a circular grating or reflective zone plate fabricated onto a flat glass substrate. The holograms used at Steward Observatory were made by etching concentric grooves into fused silica substrates and coating with reflective aluminum. The CGH patterns were fabricated using electron beam lithography that has been developed for the production of integrated circuits. The spacing of the grooves is determined analytically to synthesize a wavefront reflected by a perfect mirror. The groove depth and width are optimized to minimize fabrication costs while giving the correct intensity of the diffracted light.

0-8194-1242-2/93/$6.00

A layout of the CGH null test, shown in Fig. 1, depicts an Offner null lens[3,5] and CGH. No modifications are made to the null lens for performing this test; the null corrector tests the hologram exactly as if a real mirror was being measured. The use of the hologram to test the null corrector is surprisingly simple. The CGH is positioned at the paraxial focus of the null corrector. Once the CGH is near the correct position, the shape of the fringes in the interferometer is used to align the hologram. Since the CGH appears to the null corrector to be a complete primary mirror with the correct shape, the alignment of the hologram is exactly like that of the actual primary. The lateral translation, axial translation, and tilt of the null lens are adjusted to eliminate tilt, focus, and coma from the interferogram.

The azimuthal errors in the holograms were removed from the null lens measurements by averaging many data maps taken with the CGH at different rotational positions. When an average of many maps is taken with the CGH at equally spaced rotational positions, the non-axisymmetric errors in the CGH average out while the errors in the null lens remain. It is easy to rapidly make many measurements with the CGH because of the short optical path length.

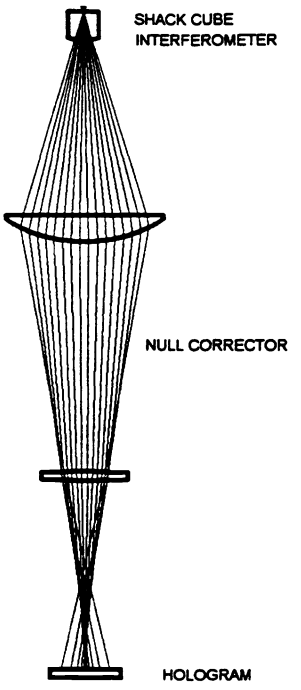

Figure 1. Layout of CGH test of null lens. The use of the CGH involves simply positioning the hologram at the correct location and making the measurement as if testing the mirror itself.

The holograms are designed to give about 4% diffraction efficiency into the desired order. This matches the intensity from the reference surface to give a high-contrast interference pattern. A pinhole positioned near the Shack cube rejects the stray orders of diffraction and lets only the desired order through. The size of the pinhole is optimized so that the area corresponding to the entire tested region of the mirror is free from spurious orders, but the spatial frequency cutoff is acceptable.

2. OPTICAL TESTING WITH COMPUTER-GENERATED HOLOGRAMS

2.1. BACKGROUND ON CGH AND OPTICAL TESTING

Optical testing of aspheric surfaces using computer-generated holograms (CGH's) has been used for over twenty years. An excellent summary of CGH optical testing is given by Loomis[6]. Some more recent work in the field is given in a thorough review by Creath and Wyant[7].

A hologram is generally used to modulate the phase or amplitude of a wavefront, causing it to propagate such that it forms a desired phase front or intensity distribution. A photographically produced hologram may be used to store and play back an existing wavefront[8]. Synthetic holograms may also be specified by a computer and written with an electronic plotter[9]. The computer-generated hologram is a diffraction grating that uses a spatial variation in ruling frequency to create a desired change in wavefront. The CGH may be interpreted as changing ray directions according to the grating equation,

$$s(\sin\theta_0 + \sin\theta_m) = m\lambda \tag{1}$$

where θ_0, θ_m = incident and diffracted angle

λ = wavelength

m = order of diffraction

s = local ruling center-to-center spacing.

Equivalently, the hologram changes the wavefront phase. When used in m^{th} order, the CGH adds m waves of optical path to the wavefront for each ruling cycle.

Optical testing with a CGH is commonly[10,11] performed using a configuration similar to that shown in Fig. 2. The spatial filter is required to block the unwanted orders of diffraction. The diverger lens need not be perfect, but only well known because the CGH will correct for the mirror-lens combination.

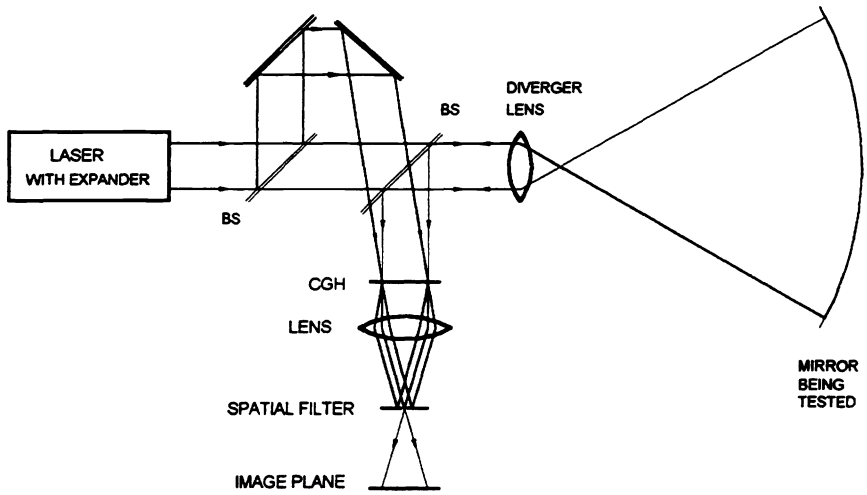

Figure 2. Modified Twyman-Green interferometer for testing an aspheric mirror with a CGH.

A large amount of tilt must be created by the CGH to cause the orders to fan out, enabling the isolation of a pure reference and pure test beam[6]. This wavefront tilt, which causes a carrier frequency in the ruling, must be three times larger than the maximum slope of the aspheric wavefront to insure complete separation of orders[12].

Since the CGH is nothing more than a pattern drawn on film or glass, its errors take the form of spatial distortion in that pattern. The magnitude of the wavefront error due to the distortion is given by the scalar product of the wavefront gradient and the vector distortion[13].

2.2 CIRCULAR HOLOGRAMS

Circular holograms have been used in optical testing and are used for the CGH null lens test. Rather than using a tilt carrier to fan out the orders laterally, the rotational CGH causes the different orders to focus at different positions along the axis. The use of circular holograms for optical testing was first demonstrated by Buynov[14]. Ichioka and Lohmann[15] discuss the use of a quadratic (focus) carrier to shift the longitudinal focus position of the unwanted orders. They used a small aperture at the focus of the desired order to restrict the interference of spurious orders to a small central area of the optic. They also showed that the actual number of fringes plotted may be less for a circular hologram than for a linear hologram. Further comparisons between circular and tilt carrier holograms are given by Mercier[16] and Mercier and Lowenthal[17].

There are several advantages of rotational holograms for testing axisymmetric optics. By preserving the axial symmetry, the hologram design and analysis are reduced from two dimensions to one. The alignment of the centered system is straightforward using conventional techniques[17]. The symmetry also allows direct certification of the hologram by measuring ring diameters[18]. For testing optics with annular apertures, the inability to test the central region is inconsequential[19]. For testing a mirror with no central obscuration, the central region generally has very little asphericity and can be tested conventionally[20].

The use of circular holograms is ideal for conditions when the desired order comes to a sharp, unaberrated focus. At this point, a small pinhole will allow the desired light cone through while blocking all other orders. Background light and spurious fringes may be further reduced by physically masking off the inner region of the light cone, corresponding to the center hole in the primary.

The size of the pinhole is optimized to reject the stray orders without limiting resolution. The pinhole is positioned at the center of curvature of the interferometer reference surface where the light comes to a sharp focus. Figure 3 shows how a stray order is blocked by the pinhole. The light from the desired order comes to a sharp focus at the pinhole. The unwanted orders are out of focus and aberrated so they do not make it through the aperture. Since an annular pupil is used, an out-of-focus stray order will cause an annular image. As long as the pinhole is smaller than the inner diameter of this annulus, the light in this stray order will be completely blocked.

The pinhole may not be made arbitrarily small however because it acts as a low-pass spatial filter with cutoff spatial frequency derived using Fourier optics[3,21]. For the null lens for the WIYN 3.5-m primary that uses a 0.332 *NA* beam, a 200-μm pinhole gives 30 cycle-per-meter resolution or 105 full cycles across the mirror diameter. This frequency optimally matches the Nyquist sampling rate determined by the digitization of 200 pixels across the mirror. This pinhole also completely rejects all but the desired orders of diffraction in the clear aperture.

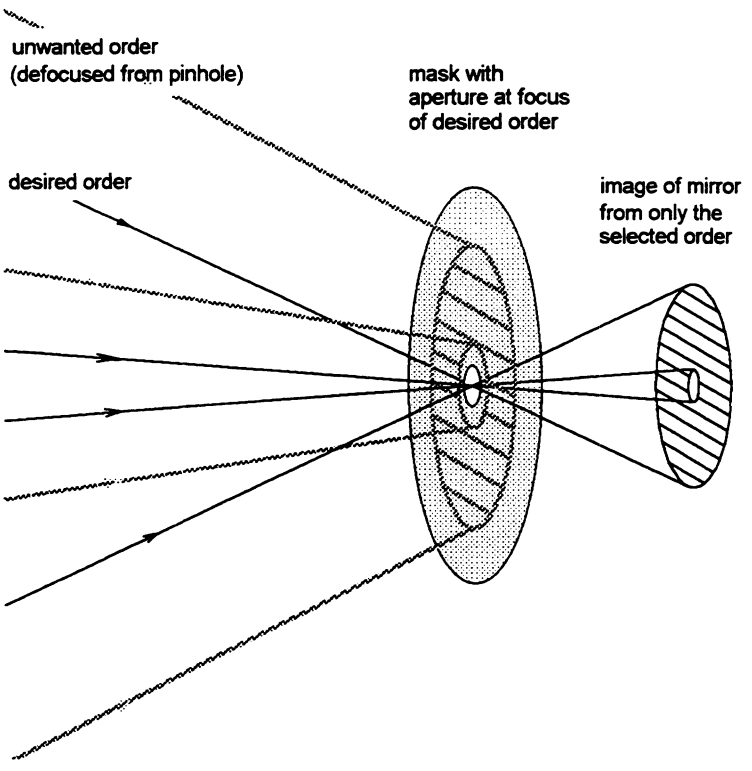

Figure 3. Rejection of stray diffraction orders. The order rejection relies on two principles. (1) The desired order comes to a sharp focus where all other orders are out of focus, and (2) An annular pupil is used. There is a central untested region that is blocked elsewhere.

3. DESIGN AND FABRICATION OF CGH FOR NULL LENS TEST

3.1. CGH DESIGN

The CGH design is defined only by the shape of the primary mirror and not any specific null lens. The radial ring positions are chosen based on an exact analytical model of the rays normal to the primary mirror[3]. The normal rays are propagated analytically to intersect a plane at the paraxial center of curvature of the mirror. The intercept positions define the mapping of the mirror position onto the hologram plane (See Fig. 4.) The path length variation across the mirror defines the hologram phase function. This model gives an exact expression for the wavefront function that the CGH must create to synthesize a perfect primary mirror. Approximations are used only for the error analysis.

The exact relationships were expanded in power series and truncated for the error analysis. The following definitions are made:

r	= radial mirror position
R	= vertex (paraxial) radius of curvature of mirror
K	= conic constant of mirror
$x(r)$	= ray intercept position on hologram corresponding to r on mirror.

The CGH is encoded by specifying a phase function for the diffraction to create. For use in the m^{th} order, this CGH will consist of one plotted fringe for every m waves in the phase function. The holograms for testing the null correctors are used in reflection, so the phase functions must be twice the OPD given above. This gives ring positions for every $m \times \lambda/2$ of the OPD.

The shape of the OPD function (see Fig. 5) looks conical with little slope change over most of the CGH. This fortunate shape allows the CGH to work with no carrier at all. The radial slope in the wavefront itself is sufficient to act as a circular carrier with ring spacing nearly constant over most of the hologram. The CGH function shown in Fig. 5 shows why the conventional method of specifying CGH functions as a power series with even terms fails to converge for designing this hologram. There is a cusp at the center that is poorly modeled using a power series with a reasonable number of terms.

Mapping of mirror to CGH

For a hologram at paraxial focus, the rays map from the mirror to the CGH according to

$$x(r) \cong \frac{-Kr^3}{2R^2}$$

OPD at CGH

The wavefront created by the CGH is approximated as

$$OPD \cong -\frac{3Kr^4}{8R^3}$$

Mapped into CGH coordinates, this takes the form below.

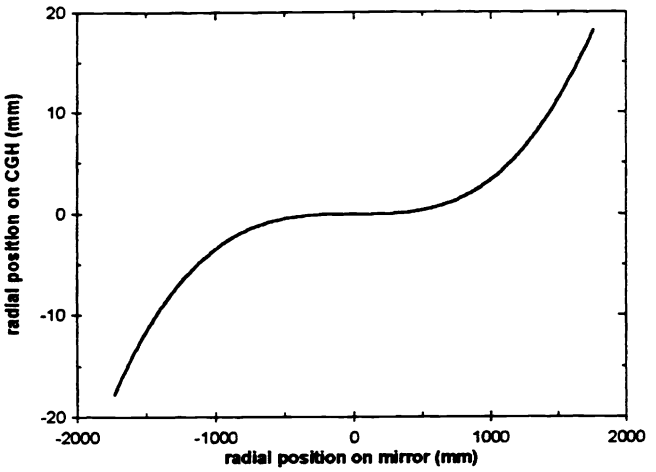

Figure 4. CGH mapping function showing the relationship between mirror position and position on hologram. This plot is for a CGH used to test a null corrector for a 3.5-m *f*/1.75 primary mirror.

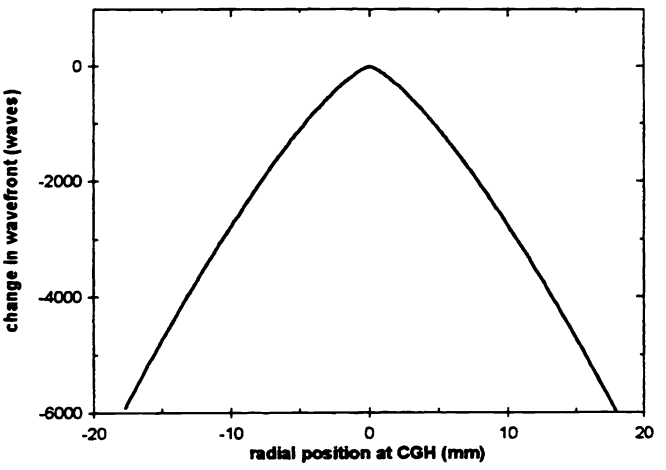

Figure 5. Wavefront phase function required of a paraxial-focus CGH to test a null corrector for a 3.5-m *f*/1.75 primary mirror.

It is interesting that this OPD for the null corrector test has minus three times the aspheric deviation of the primary mirror,

$$Surface\ Asphere \cong \frac{Kr^4}{8R^3} \tag{2}$$

The surface aspheric departure represents the surface deviation from a reference sphere centered at paraxial focus. The above OPD is the path difference for a normal ray that intersects the CGH plane.

3.2. CGH FABRICATION

The fabrication of holograms using electron beam lithography is now quite common[11,22]. There are firms that specialize in the encoding and printing of CGH's. They have software that evaluates a phase function, usually specified with polynomial coefficients, to create a data file that will drive the plotter. This involves approximating the continuous fringes as chains of trapezoids that the plotter can directly write[23]. The error in the approximation is negligible if small enough trapezoids are used.

The fabrication of the holograms for testing the null correctors at SOML uses electron beam lithography to write a master, which is then printed to the final substrate. This allows the usual practice of writing the master onto a thin, pre-coated glass slide, while the final CGH is on a thick, optically flat glass substrate. This method can severely limit the accuracy of the CGH if the printing is flawed. For this reason, it may be preferable to have the final CGH written directly by the e-beam writer.
The CGH is contact printed by holding the master in direct contact with the photoresist-coated blank and exposing with collimated light. The master can be certified as accurate to ±0.15 μm, and the errors from well-controlled contact printing are less than ±0.1 μm[24]. Since it is difficult to verify the final printing to sub-micron accuracy, an error in the printing could go undetected, leading to an inaccurate optical test.

By using the CGH in third order, the number of rings required to test a null lens is reduced and the smallest feature size is increased by a factor of three. This makes the part easier and less costly to fabricate. To get the desired diffraction efficiency from the third order, the CGH is made into a pure phase element by etching grooves into the glass and coating the entire surface with reflective aluminum.

4. ERROR ANALYSIS

The error terms, as analyzed in this section, originate from three sources: the CGH itself, the implementation of the test, and the analysis of the data. These terms are described and analyzed below. The derivations are given more completely elsewhere[3].

4.1. ERRORS FROM FABRICATION OF CGH

The most obvious errors in the CGH null lens test come from the errors in the CGH itself. All possible error sources are evaluated and added to estimate the uncertainty in the CGH. The CGH errors can come from the substrate surface figure, e-beam writing errors, printing to the final substrate, or phase etching. They are separated as either figure or hologram errors depending on whether the phase error is caused by the surface reflection or diffraction. The figure errors affect the wavefront from all diffracted orders equally, and the effects of the hologram distortion errors are proportional to the order number. The hologram distortion does not affect the wavefront from the zero-order specular reflection. However, the variations in etch width and depth strongly affect the zero-order reflection, but have a minimal effect on the other orders.

4.1.1. SURFACE FLATNESS

The figure error in the hologram surface adds a phase error to the diffracted wavefront that is twice the surface error of the CGH. The wavefront phase errors due to small-amplitude low-frequency figure errors are identical for all diffracted orders. In the absence of other errors, this fact would enable the direct measurement of the figure errors using a Fizeau interferometer with a flat reference. The measured figure errors could then be subtracted from the null lens measurement. However, variations in the etch depth and duty cycle cause irregularities in the zero-order or specular wavefront that are much larger than those in the non-zero-order diffracted wavefronts. The flatness of the CGH substrate must be measured *before* the hologram is applied. The error in the null lens test due to the CGH surface flatness is quite small. The substrates are specified flat to λ/20 at 546 nm and the majority of this error is likely to be astigmatism that is removed from the null lens measurement by rotating the hologram.

4.1.2. HOLOGRAM DISTORTION

The most severe errors in this test are the hologram errors consisting of distortion in the ruling pattern. The distortion may be caused by limitations in the e-beam writing or in the printing onto the final substrate. Distortion causes an error in the diffracted wavefront, approximated for the null lens test as

$$\Delta W = \frac{2\varepsilon_x r}{R} \tag{3}$$

where, ΔW = wavefront error (twice surface error in measurement)
ε_x = radial CGH error (actual radial position of groove - desired position)

r = virtual radial position in mirror coordinates
R = radius of curvature of primary mirror.

The first order approximation is independent of the order m and wavelength.

The effect of the CGH error for the null lens test is analyzed by making the above approximations for W(r) and $x(r)$. The most significant radial error in the CGH is the linear scale of the hologram. A scale error C gives a shift in the pattern ε_x proportional to radial position, $\varepsilon_x = Cx$.

This causes the diffracted wavefront to have an error, which is simply spherical aberration W_{040},

$$\Delta W = \frac{2r}{R} C\left(-\frac{Kr^3}{2R^2}\right) = -C\frac{Kr^4}{R^3}. \tag{4}$$

The conic constant change in the primary mirror that would cause this W_{040} is

$$\Delta K = \frac{4R^3}{r^4} \times W_{040} = -4K \times C. \tag{5}$$

This result is interesting; it is only the linear component of the CGH distortion, which is a scale error, that causes an error in the measured conic constant.

The magnitude of the hologram errors is estimated from knowledge of the encoding, writing, and printing process accuracy. The CGH encoding is performed with sufficient resolution to insure digitization errors less than the e-beam pixel size. The e-beam writers are verified to be accurate to ±0.15 μm. The accuracy of the printing depends on the method used and the expertise of the technician.

The form of the hologram errors determines the type of wavefront errors induced. Most of the encoding and writing errors occur over small spatial scales causing high frequency errors that are filtered out[25]. Since azimuthal errors average out when rotating the CGH, the error budget must only include spherical aberration. The magnitude of the third-order spherical aberration (which has a fourth order dependence on r) is estimated by assuming the distortion can cause pure W_{040}. This translates into a scale error given by the ratio of the maximum shift ε_x over the radius of the CGH. The resulting wavefront error is given by Eq. (4).

The higher-order spherical aberration is assumed to be much smaller than the low-order error described above. The holograms are written and printed using equipment for making integrated circuits, so the higher-order writing and printing errors should have no tendency to be axisymmetric. An upper limit on the magnitude of the higher-order errors may be obtained assuming all of the grating error occurs where period is minimal. Assuming the maximum distortion occurs near the edge of the hologram, the maximum wavefront error ΔW_{max} is given by

$$\Delta W_{max} = \frac{2r_{max}}{R}\left(1 + \frac{Kr_{max}^{\ 2}}{2R^2}\right) \times \varepsilon_{max}. \tag{6}$$

For the CGH null lens test for a 3.5-m f/1.75 primary mirror, a 0.2 μm maximum hologram error can cause a maximum wavefront error of 56 nm at the edge of the clear aperture.

4.1.3. ETCHING ERRORS

Variations in the depth of the etched grooves and the ruling duty cycle must also be considered as potential error sources. The variations in duty cycle or errors in the width of the etched grooves cause only variation in diffraction efficiency for the non-zero diffracted orders. These errors do cause phase variations for the zero order diffraction. The etch depth variations cause

phase variations for all orders. For grooves nominally λ/4 deep, the wavefront variations are equal to the variations in etch depth. Groove depth variation of ±2% will give wavefront errors of ±λ/200.

4.2. ERRORS FROM USE OF CGH

A CGH manufactured without figure or writing errors does not guarantee a perfect null lens test. The test of the null corrector will only give a null result for a flawless null lens and CGH that are designed for the same radius of curvature, conic constant, and wavelength of light. Also, a change in the temperature of the CGH will cause it to expand and induce spherical aberration. Since the CGH emulates a perfect primary mirror, the alignment does not significantly affect the test accuracy. Noise in the measurements due to vibration, seeing, random electronic noise, and digital round-off errors are negligible in the average of many measurements.

The analysis of these effects is handled by treating the CGH as a plane surface that introduces a wavefront change of twice the single-pass OPD. This is a sensible thing to do because the ruling is known to introduce three waves of OPD per ring into the third order. Since the measurements are performed in terms of surface variations, this OPD is treated using an effective surface function S_{CGH} which is exactly half of the wavefront change. This surface function is equal to the single-pass OPD given above,

$$S_{CGH} = -\frac{3Kr^4}{8R^3} \tag{7}$$

where r is the virtual position at the mirror.

The null lens is designed to measure a mirror with a given radius R and conic constant K, but it will yield a null test for a family of surfaces. The actual shape of the surface depends on the distance to the primary being tested. The CGH test measures only the null corrector, so the measured errors must assume an R of the primary mirror. Ideally, the CGH is fabricated for exactly the R of the primary. If it is not, corrections to the data must be made for the known differences.

4.2.1. RADIUS OF CURVATURE ERROR

If the CGH and the null lens are designed for different values of R, the primary radius of curvature, the CGH null lens test will show spherical aberration. The relationship between the spherical aberration or conic constant change dK, and dR is shown to be[3]

$$\frac{dR}{R} = -\frac{dK}{K}. \tag{8}$$

So a CGH with $dR = 0.0001R$ will cause spherical aberration that has the same effect as a conic constant change of +0.0001 for a parabola.

4.2.2. ERROR IN LASER WAVELENGTH

Since diffraction is a wavelength dependent effect, a change in the laser wavelength would cause an error in the measurement. The wavelength of the laser light is dependent on the frequency of the transition for stimulated emission and the refractive index of the air. Using an unstabilized, single-mode gas laser, the frequency can take any value within the Doppler-broadened width of the gain curve. The refractive index of the air is easily calculated based on the temperature and pressure.

The function S_{CGH} is the effective surface corresponding to three waves per cycle at the design wavelength. So S_{CGH} in units of length is really a phase function times the wavelength of the light used. A change in the wavelength must cause a proportional change in S_{CGH},

$$\Delta S_{CGH} = S_{CGH}\frac{\Delta\lambda}{\lambda} = -\frac{3Kr^4}{8R^3}\frac{\Delta\lambda}{\lambda}. \tag{9}$$

This leads to

$$\Delta K = 3K\frac{\Delta\lambda}{\lambda}. \tag{10}$$

4.2.3. ALIGNMENT OF CGH TO NULL LENS

The procedure for aligning the CGH to the null lens is identical to the alignment for the null test of primary mirrors. The lateral translation, axial translation, and tilt of the null lens are adjusted to eliminate tilt, focus, and coma from the interferogram. This was derived analytically[3] and verified experimentally. The alignment is easily performed to about an eighth of a fringe and the rest is subtracted in software.

4.2.4. RANDOM MEASUREMENT ERRORS

The individual measurements of the CGH have small errors due to environmental effects, electronic noise, digital sampling, and phase calculation errors. These errors become negligible in the average of many measurements since the errors are small in amplitude and uncorrelated. The environmental effects, caused by air motion in the optical path and vibration, are much smaller for the CGH test than they are for the test of the primary mirror since the path length is so much shorter for the CGH test. For a null lens measurement consisting of 15 azimuthal rotations, 5 maps per angle, and 0.02λ rms random errors, the random component of error in the average is less than 1.5 nm rms, which is negligible.

4.3. ERRORS IN DATA REDUCTION

The last remaining type of error is due to possible errors in the interpretation of the data. This type of error is minimized for the null test -- a null result is absolute and requires no interpretation. The actual errors in the null lens and the CGH result in a measured figure that must be evaluated. Also, known errors in the CGH that are subtracted from the data cause an uncertainty in the final map from both the CGH errors and the mapping between these errors and the measured data.

The errors in the CGH are calculated in the coordinates at the real mirror. To subtract these from the data, the errors must be transformed into the data coordinates. This transformation requires knowing the imaging distortion of the null corrector and the exact relationship between the edge of the data and the edge of the mirror. The imaging distortion of the null lens is measured to about ±0.5% and the edge is determined to within ± 1 pixel. A computer program was written to remap the CGH errors according to the imaging distortion, and then fit Zernike polynomial coefficients using least squares. The fitting error due to distortion was directly assessed by simulating errors in the mapping function. The uncertainty in mapping the CGH error is independent of the uncertainty in the CGH error itself.

5. ERROR ANALYSIS FOR NULL LENS TEST FOR 3.5-m *f*/1.75 PRIMARY MIRRORS

Two null correctors for 3.5-m *f*/1.5 primary mirrors were measured using the holographic test. The results showed the conic constants of the null correctors to be correct within the measurement uncertainty of ±78 ppm. The error terms that comprise the measurement uncertainty originate from three sources: the CGH itself, the implementation of the test, and the analysis of the data. A single error analysis for two null lens tests was performed taking the worst case from both tests for each error term.

5.1. UNCERTAINTIES IN NULL LENS TEST

The errors in the hologram come from the surface figure, groove pattern distortion, and etch depth variations. The substrates were specified to be flat to λ/20 P-V. The component of this error that causes pure third-order spherical aberration (fourth-order dependence on *r*) in the null lens test has a cone-shaped appearance[3,4]. For the error analysis, it was assumed that this component of the figure error is less than λ/20. The e-beam writer has errors as large as ±0.15 μm and printing errors can be as large as ±0.2 μm. The encoding and digitization errors are not considered because they cause high-frequency errors that do not affect the conic constant. The grooves were specified to be etched to a depth of λ/4 with less than 5% depth variation over the entire aperture. The error analysis assumes the worst case of 5% depth variation causing pure spherical aberration. The gross errors discussed below are not included here because they cause phase discontinuities that are easily recognizable.

The uncertainty of the laser wavelength has several components. The uncertainty in the laser frequency is determined by the width of Doppler-broadened gain of the neon transition. The frequency of a single-mode, unstabilized HeNe laser will be 473612 ± 1 GHz[26]. Errors in the refractive index of air caused by the uncertainty in the temperature and pressure measurement will cause an error in the wavelength. The thermal expansion of the fused silica holograms will also cause measurement errors proportional to the temperature difference between fabrication and use.

The errors in data analysis are due to the uncertainty of the Zernike polynomial fit to the data and the uncertainty of the mapping between the mirror and the image. The Zernike polynomial fit of spherical aberration is estimated to be uncertain to ±0.003λ. An error in the distortion coefficient of 0.5% would cause an error of 0.0001λ in the 0.06λ spherical aberration correction to the WIYN data. A 1% error in the definition of the edge, corresponding to 1 pixel, would cause an additional 0.0024λ error.

These errors are summarized in Table 1 in terms of the uncertainty in the Zernike spherical aberration coefficient *Z8* and the conic constant dK. The estimated uncertainty of the test is found by taking a root-sum-square (RSS) of the independent terms.

Table 1. Error budget for CGH null lens measurements for 3.5-m *f*/1.75 primary mirrors.

Error term	Value ± uncertainty	±Z8 (waves)	±dK (ppm)
Manufacturing errors			
write errors	±0.15 μm over 20 mm radius	0.0054	32
print errors	±0.2 μm over 20 mm radius	0.0072	43
substrate flatness	λ/20	0.0083	50
etch depth variations	5% of λ/4	0.0010	6
Errors in use			
CGH temperature	21 ± 3° C	0.0014	8
laser frequency	473612 ± 1 GHz	0.0011	6
air pressure	697 ± 5 mm Hg	0.0010	6
air temperature	21 ± 2° C	0.0011	6
Data analysis error			
mapping distortion error	6.7 ± 0.5 %	0.0001	1
edge definition error	1 pixel	0.0024	14
fit error ΔZ8		0.0030	18
RSS		**0.0131**	**78**

A gross flaw that appears as a sharp step in the diffracted wavefront has been present in several holograms. This error, which occurs during the replication of the e-beam written master to the final substrate, is not treated in this analysis. A hologram with this printing error has the well-defined step that makes the hologram unusable.

5.2. RESULTS FROM TESTING TWO NULL CORRECTORS

The two null correctors for 3.5-m primary mirrors, for the ARC and WIYN telescopes, were measured at 11 and 15 equally spaced rotational positions. Small corrections to the data were required to compensate for changes in wavelength and radius of curvature between the hologram and null corrector designs. The CGH measurement of the ARC null lens found -11.4 nm spherical aberration corresponding to a conic constant error of -72 ppm. The measured spherical aberration in the WIYN null corrector was only -3 nm, corresponding to a conic constant error of -19 ppm. These are within the expected errors of 80 ppm, as determined by the null corrector tolerance analysis.

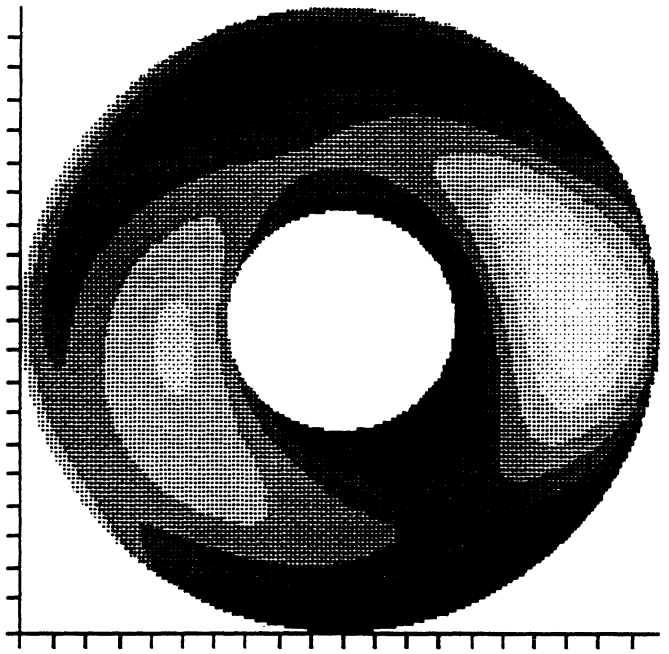

Figure 6. Contour map showing measured null lens error of 7.6 nm rms for ARC primary mirror as represented by a 36-term Zernike polynomial fit. Surface contours are plotted at 5 nm intervals over a range from -20 nm to 20 nm.

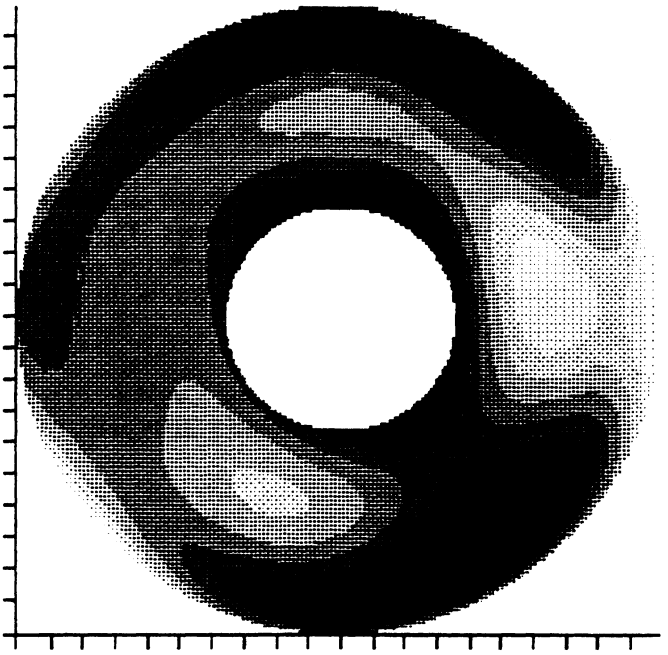

Figure 7. Contour map showing measured null lens error of 5.1 nm rms for WIYN primary mirror. The surface errors, computed from a 36-term Zernike fit to the data, are plotted with contours at 3 nm intervals over a range from -12 nm to 12 nm.

A visual comparison between measurements of the ARC null lens (Fig. 4) and the WIYN null lens (Fig. 5) shows a strong correlation. This is expected because the largest source of error in the null lenses, the refractive index inhomogeneity, is the same for both systems. The alignment errors are expected to be different.

6. CONCLUSION

A null lens test using a computer-generated hologram is presented including a background on CGH testing, a detailed description of the CGH null test design and optimization, and a thorough error analysis. This new test works by using the null corrector to test a small circular hologram or zone plate that is placed at the paraxial focus of the null lens. The zone plate diffracts light back into the null corrector that precisely matches the light that would be reflected by a perfect primary mirror many meters away. The CGH null lens test is used to certify a critical and precise instrument, so a thorough error analysis has been performed. The test has three types of error sources: errors in the CGH, errors in the implementation of the test, and errors in the interpretation of the results. An effort has been made to understand and minimize all three types of errors.

The test was performed on two null correctors for 3.5-m mirrors, and it verified the null correctors as having the correct conic constants within the measurement uncertainty of ±78 ppm.

ACKNOWLEDGMENTS

This research was part of the author's Ph. D. dissertation in Optical Sciences at the University of Arizona under Prof. Roger Angel.

REFERENCES

1. L. Allen, J. R. P. Angel, J. D. Mongus, G. A. Rodney, R. R. Shannon, C. P. Spoelhof, "The Hubble Space Telescope optical systems failure report," NASA Report. Nov., 1990.
2. R. N. Wilson, F. Franza, L. Noethe, and G. Andreoni, "Active optics IV. Set up and performance of the optics of the ESO New Technology Telescope (NTT) in the observatory," J. Mod. Optics **38**, 219-243 (1991).
3. J. H. Burge, *Advanced Techniques for Measuring Primary Mirrors for Astronomical Telescopes,* (Ph. D. Dissertation, Optical Sciences, University of Arizona, 1993).
4. J. H. Burge, "Certification of null correctors for primary mirrors," in *Advanced Optical Manufacturing and Testing IV*, J. Doherty, ed., Proc. SPIE **1994**, in press (1993).
5. A. Offner, "A null corrector for paraboloidal mirrors," Appl. Opt **2**, 153-155 (1963).
6. Loomis, J. S., "Computer-generated holography and optical testing," Opt. Eng. **19**, 679-685 (1980).
7. K. Creath and J. C. Wyant, "Holographic and speckle tests," in *Optical Shop Testing*, D. Malacara, Editor (Wiley, New York, 1992) pp. 599-651.
8. E. N. Lieth and J. Upatnieks, "Reconstructed wavefronts and communication theory," J. Opt. Soc. Amer. **52**, 1123-1130 (1962).
9. B. R. Brown and A. W. Lohmann, "Complex spatial filtering with binary masks," Appl. Opt. **5**, 967-969 (1966).
10. J. C. Wyant and V. P. Bennett, "Using computer-generated holograms to test aspheric wavefronts," Appl. Opt. **11**, 2833-2839 (1972).
11. S. M. Arnold, "How to test an asphere with a computer-generated hologram," in *Holographic Optics: Optically and Computer Generated,* I. N. Cindrich and S. H. Lee, Editors, Proc. SPIE **1052**, 191-197 (1989).
12. T. Yatagai. and H. Saito, "Dual computer-generated holograms for testing aspherical surfaces," Opt. Acta **26**, 985-993 (1979).
13. A. F. Fercher, "Computer-generated holograms for testing optical elements: error analysis and error compensation," Opt. Acta **23**, 347-365 (1976).
14. G. N. Buynov, N. P. Larionov, A. V. Lukin, K. S. Mustafin, and R. A. Rafikov, "Holographic interferometric inspection of aspherical surfaces," *Optical Technology* **38**, 194-197 (1971).
15. Y. Ichioka and A. W. Lohmann, "Interferometric testing of large optical components with circular holograms," Appl. Opt. **11**, 2597-2602 (1972).
16. R. Mercier, "Holographic testing of aspheric surfaces," in *First European Conference on Optics Applied to Metrology*, M. Grosmann and P. Meyrueis, Editors, Proc SPIE **136**, 208-214 (1977).
17. R. Mercier and S. Lowenthal, "Comparison of in-line carrier frequency holograms in aspheric testing," Opt. Comm. **33**, 251-256 (1980).
18. A. V. Lukin and K. S. Mustafin, "Holographic methods of testing aspherical surfaces," Sov. J. Opt. Tech. **46**, 237-244 (1979).
19. G. I. Aver'yanova, N. P. Larionov, A. V. Lukin, K. S. Mustafin, and R. A. Rafikov, "The testing of large aspherical surfaces by means of synthetic circular holograms," Sov. J. Opt. Tech. **42**, 347-349 (1975).
20. N. P. Larionov, A. V. Lukin, and R. A. Rafikov, "Testing of aspherical surfaces by means of axial synthesized holograms," Sov. J. Opt. Tech. **47**, 667-670 (1980).
21. J. W. Goodman, *Introduction to Fourier Optics*, (McGraw-Hill, San Francisco, 1968).
22. K. S. Urquhart, S. H. Lee, C. C. Guest, M. R. Feldman, and H. Farhoosh, "Computer aided design of computer generated holograms for electron beam fabrication," Appl. Opt. **28**, 3387-3396 (1989).
23. S. M. Arnold, "Desktop computer encoding of electron-beam written holograms," in *Computer-Generated Holography II,* S. H. Lee, Editor, Proc. SPIE **884**, 23-26 (1988).
24. P. N. Everett, "Metrology of lithographic features: balanced illumination eliminating diffractive bias," Appl. Opt. **32**, 1216-1224 (1993).
25. A. D. Kathman, R. L. Clark, H. J. Rogers, M. G. Temmen, P. E. Fileger, and C. F. Hester, "Wave optics modeling of CGH designs," in *Computer-Generated Holography II,* S. H. Lee, Editor, Proc. SPIE **884**, 13-22 (1988).
26. K. D. Mielenz, K. N. Nefflen, W. R. C. Rowley, D. C. Wilson, and E. Engelhard, "Reproducibility of helium-neon laser wavelengths at 633 nm," Appl. Opt. **7**, 289-292 (1968).